

Fig. 6.32. Comparison of observed and predicted rigidity at seamounts and oceanic islands that form on > 80-Ma oceanic lithosphere. The observed values are based on Table 6.1 and have been colour coded according to the age of the lithosphere at the time of loading. The predicted curves are based on a multilayered viscoelastic plate model with  $E_c = 120 \text{ kJ mol}^{-1}$  and  $\eta_{ref} = 10^{20} \text{ Pa s}$  and an age of the lithosphere at the time of loading,  $t_{sf} - t$ , of 30, 70, 110 and 150 Ma. Reproduced from Fig. 10 of Watts and Zhong (2000).

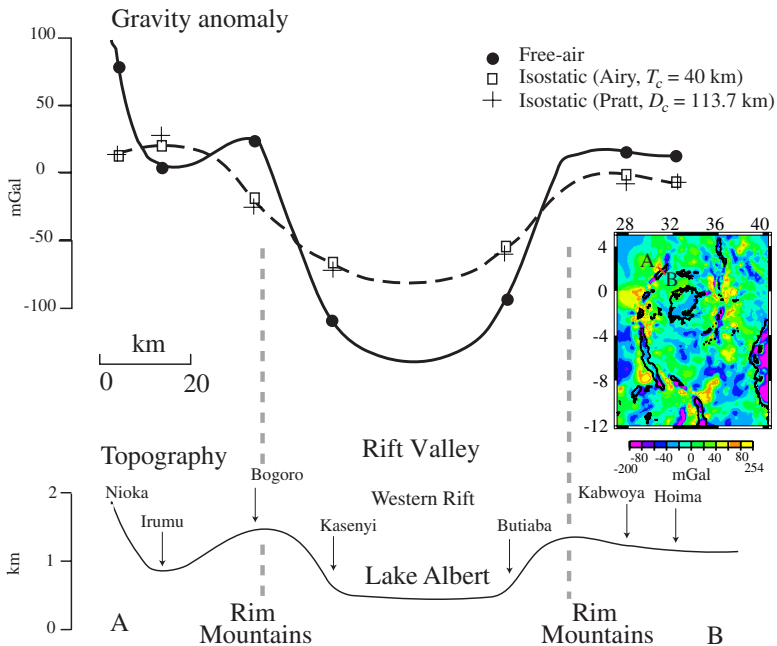


Fig. 7.1. Topography, free-air, and Airy ( $T_c = 40 \text{ km}$ ) and Pratt ( $D_c = 113.7 \text{ km}$ ) isostatic gravity anomaly profile of Lake Albert in the East Africa Rift system. Based on data in Table XXII of Bullard (1936). Inset shows a free-air gravity anomaly map of the East Africa region.